ACS APPLIED MATERIALS & INTERFACES
Research Article
www.acsami.org

Facile Fabrication of Magnetic Chitosan Beads of Fast Kinetics and High Capacity for Copper Removal

Wei Jiang, Wenfeng Wang, Bingcai Pan,* Quanxing Zhang, Weiming Zhang, and Lu Lv*

State Key Laboratory of Pollution Control and Resources Reuse, School of the Environment, Nanjing University, Nanjing 210023, People's Republic of China

Supporting Information

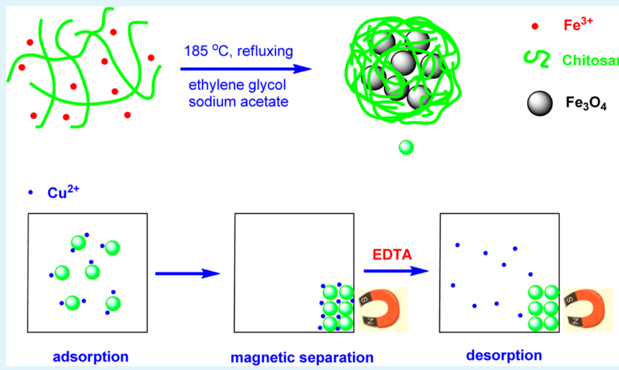

ABSTRACT: In this study, magnetic chitosan (CS) beads of ~200 nm in diameter were successfully prepared by a facile one-step method. The resultant composite Fe_3O_4−CS was characterized using transmission electron microscopy (TEM), X-ray powder diffraction (XRD), thermogravimetric analysis (TGA), and Fourier transform infrared spectroscopy (FTIR). Its adsorption toward Cu(II) ions was investigated as a function of solution pH, CS dosage, Cu(II) concentration, and contact time. The maximum capacity of Fe_3O_4−CS was 129.6 mg of Cu(II)/g of beads (617.1 mg/g of CS). More attractively, the adsorption equilibrium could be achieved within 10 min, which showed superior properties among the available CS-based adsorbents. Continuous adsorption−desorption cyclic results demonstrated that Cu(II)-loaded Fe_3O_4−CS can be effectively regenerated by ethylenediaminetetraacetic acid (EDTA) solution, and the regenerated composite beads could be employed for repeated use without significant capacity loss. Additionally, Fe_3O_4−CS beads can be readily separated from water within 30 s under a low magnetic field (<0.035 T).

KEYWORDS: *magnetic chitosan beads, Fe_3O_4, Cu(II), fast removal*

1. INTRODUCTION

Exposure to toxic heavy metals even at trace levels is a risk for humans. Nowadays, various techniques have been developed to respond to heavy metal pollution in water, such as chemical precipitation,[1] ion exchange,[2] adsorption,[3] and electrodialysis.[4] While effective, they are very often costly and time-consuming. As for adsorption, how to develop a specific adsorbent with high capacity and low cost is an interesting but still challenging task. Biosorption seems to be an attractive approach because the biosorbent is readily available, economic, and environmentally compatible.[5,6] Among the currently available biosorbents, chitosan (CS) is considered as a promising choice for effectively removing or even recovering target heavy metals from water. CS contains abundant hydroxyl and amino groups on the chain backbone. It can adsorb 5−6 times greater amounts of metals than chitin because of the chelating effect. Now various CS-based adsorbents have been obtained for removal of toxic heavy metals, such as Cr(V), Hg(II), and Cu(II).[7−10]

However, as limited by the three-dimensional ordered crystal structure of natural CS,[11] a considerable amount of the functional groups of CS cannot be accessible for heavy metal sequestration. It is still an urgent task to further improve the capacity of CS-based adsorbents. Lowering the size of CS even to the nanoscale level is expected to result in an increasing amount of functional groups exposable for heavy metal adsorption.[9] To facilitate the separation and/or recycling of fine CS particles, in the past few years, scientists tried to coat them onto the magnetic particles to obtain magnetic composite adsorbents and an external magnetic field could result in a fast and feasible separation.[12−15] Liu et al. reported their recent study on the fabrication of magnetic cellulose−CS hydrogel beads[16] by using ionic liquids. They observed that the resultant composite exhibited a much higher capacity than other reported CS-based adsorbents for Cu(II) removal. Unfortunately, because of the large magnetic beads (~20 μm in diameter), more than 10 h is required for adsorption equilibrium, thus greatly limiting their applicability. Grafting CS chains to the surface of Fe_3O_4 nanoparticles could result in nanosized magnetic CS beads of satisfactory metal adsorption in terms of capacity and kinetics.[17] However, their preparation is generally complicated, including at least three steps,[12,17,18] e.g., synthesis and surface modification of Fe_3O_4 nanoparticles and grafting CS chains to their surface.

Herein, we reported a facile one-step method to *in situ* prepare nanomagnetic CS particles. The resulting Fe_3O_4−CS composite was well-characterized, and its adsorption toward copper ions was examined as a function of solution pH, CS

Received: December 4, 2013
Accepted: February 13, 2014
Published: February 13, 2014

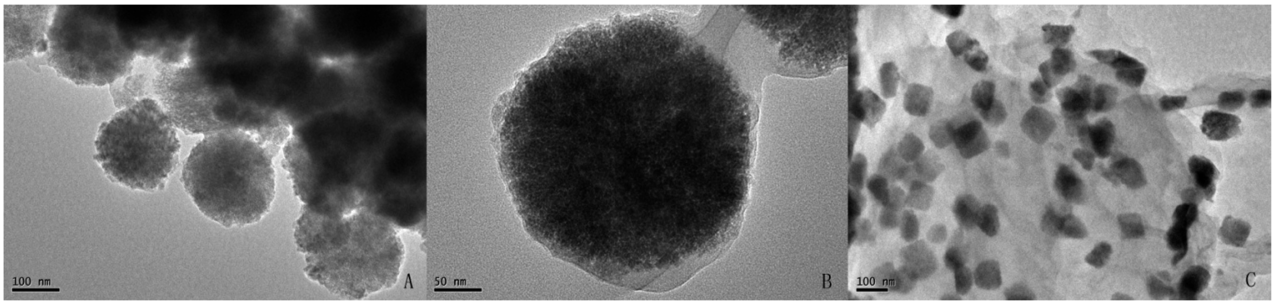

Figure 1. TEM image of (A and B) Fe_3O_4−CS-1 and (C) Fe_3O_4−CS-2.

dosage, contact time, and adsorbate concentration. Also, the reusability of Fe_3O_4−CS was evaluated as well as its separation in a low magnetic field.

2. MATERIALS AND METHODS

2.1. Materials. CS (80−95% deacetylation, with a viscosity average molecular weight of 3.0×10^5 g mol^{-1}), $FeCl_3 \cdot 6H_2O$, sodium acetate, sodium nitrate, ethylene glycol copper nitrate, hydrochloric acid, and sodium hydroxide were purchased from Zhongdong Chemical Reagent Co. (Nanjing, China). Stock solutions of Cu(II) were prepared by dissolving appropriate $Cu(NO_3)_2 \cdot 3H_2O$ in distilled water (DI). Also, all of the reagents were analytical-reagent-grade, and all solutions were prepared with DI without further purification.

2.2. Preparation of Fe_3O_4−CS and Fe_3O_4. The magnetic particles Fe_3O_4−CS and Fe_3O_4 could be obtained through a modified solvothermal reduction approach.[19−22] In detail, $FeCl_3 \cdot 6H_2O$ (3.60 g) was dissolved in ethylene glycol (80.0 mL) to form a clear solution, followed by the addition of the desired amount of CS powder. Afterward, the sodium acetate (12.0 g)−ethylene glycol (20 mL) solution was added dropwise into the aforementioned mixture, where sodium acetate could provide elemental oxygen for the formation of Fe_3O_4 and ethylene glycol served as a reductant to favor the formation of Fe_3O_4, instead of Fe_2O_3.[20] Then, the mixture was stirred vigorously for 30 min, heated to 185 °C gradually in an argon atmosphere, and maintained at 185 °C for 48 h. Similarly, the argon atmosphere is required to achieve a reduction environment for the formation of Fe_3O_4. After magnetic separation, the precipitations were washed several times with ethanol and water and dried at 50 °C in vacuum for 24 h and we obtained the composite Fe_3O_4−CS. According to the mass of CS added (1.0, 2.0, and 3.0 g), the obtained magnetic nanoparticles Fe_3O_4−CS were marked as Fe_3O_4−CS-1, Fe_3O_4−CS-2, and Fe_3O_4−CS-3, respectively. Fe_3O_4 was synthesized approximately based on the same method as Fe_3O_4−CS, except for the absence of CS.

2.3. Characterization. TEM images of Fe_3O_4−CS were taken with a scanning electron microscope (type JEM-200CX, JEOL Co., Japan). The content of CS in the test sample was analyzed by a thermogravimetric analyzer (type Pyris1 DSC, PerkinElmer, Waltham, MA) in a nitrogen atmosphere (10 cm^3 min^{-1}) at a scanning rate of 20 °C min^{-1}. The crystalline type of the Fe_3O_4−CS and Fe_3O_4 nanoparticles was characterized by powder X-ray diffraction (XRD, X'TRA, ARL Co., Switzerland). The FTIR spectra of the samples were recorded using a Fourier transform infrared spectrometer (NEXUS870, Thermo Fisher Scientific, Waltham, MA). All of the samples were prepared as potassium bromide tablets, and the range of the scanning wave numbers was 400−4000 cm^{-1}. A vibrating sample magnetometer (type 7400, Lakeshore Cryotronic) was employed to characterize the magnetic properties of magnetic CS beads at room temperature. Dynamic light scattering (DLS) was conducted using a Malvern Zetasizer 3000 HSa under the following conditions: T, 25.0 °C; aqueous suspension; reference index fluid, 1.330; angle, 90.00°; and wavelength, 660.0 nm. X-ray photoelectron spectroscopy (XPS) analysis was performed on a PHI 5000 Versa Probe (ULVAC-PHI, Japan) spectrometer with a Kα X-ray source (1468.6 eV of photons), operated at 15 kV and 10 mA. To calibrate the binding energy (BE) of the spectra, it was performed with the C 1s peak of the aliphatic carbons at 284.6 eV. The full width half maximum was maintained at 1.45, and the software XPSPEAK 4.1 and Origin 8.0 were used to fit the XPS spectra peaks.

2.4. Batch Cu(II) Adsorption. To examine the influence of solution pH on Cu(II) adsorption by Fe_3O_4−CS, the initial solution pH_i was adjusted in the range of 2.0−6.0 and the Cu(II) solution was 50 mg/L. A total of 50 mg of Fe_3O_4−CS was added to 100 mL of Cu(II) solution under continuous stirring at 25 °C for 12 h. The initial and final Cu(II) concentrations were analyzed with an atomic absorption spectrophotometer (AA-7000, Shamadzu, Japan). The amount of adsorption, q (mg/g), was calculated on the basis of the mass balance. As for the adsorption isothermal experiment, the initial Cu(II) ranged from 10 to 1200 mg/L.

2.5. Adsorption Kinetics. The adsorption experiments were also conducted at 25 °C and pH 5. The initial Cu(II) concentration of solution is 30.0 mg/L, and the volume is 1000 mL. A total of 500 mg of Fe_3O_4−CS-1 was added to Cu(II) solution under continuous stirring. At the designed time intervals, 2 mL of solution was sampled and filtered using a 0.22 μm membrane to determine the Cu(II) concentration by atomic absorption spectroscopy (AAS).

2.6. Desorption and Cyclic Adsorption. The Cu-preloaded Fe_3O_4−CS magnetic nanoparticles were separated from the batch adsorption runs and mixed with 10 mL of 0.01 M disodium salt of ethylenediaminetetraacetic acid (Na_2EDTA), where Cu(II) was desorbed from the solid. Six consecutive cycles of adsorption−desorption runs were carried out to test the reusability of the composite material. For each cycle, 100 mL of Cu(II) solution (30 mg/L, pH 5.0) was employed for Fe_3O_4−CS adsorption for 3 h and then desorbed with 10 mL of 0.01 M Na_2EDTA solution for 3 h. After each cyclic run, Fe_3O_4−CS was magnetically separated and washed thoroughly with DI.

3. RESULTS AND DISCUSSION

3.1. Characterization. Magnetic CS nanoparticles were subjected to thermogravimetric analysis (TGA). Results (see Figure S1 of the Supporting Information) indicated that the CS content of Fe_3O_4−CS-1, Fe_3O_4−CS-2, and Fe_3O_4−CS-3 was about 21, 36, and 36%, respectively. The typical TEM images of two Fe_3O_4−CS samples were shown in Figure 1, and those of Fe_3O_4−CS-3 and the Fe_3O_4 particles are depicted in Figure S2 of the Supporting Information. The resultant Fe_3O_4−CS-1 was spherical, with the average diameter of around 200 nm, and Fe_3O_4 nanobeads (black region) were coated inside CS (shadow region) well (panels A and B of Figure 1). As for Fe_3O_4−CS-2 and Fe_3O_4−CS-3, they were irregular in shape (Figure1C), and the Fe_3O_4 nanoparticles were dispersed in a continuous CS phase. Such different morphology of both samples may be attributed to the different dosages of CS during preparation. XPS spectra of Fe_3O_4−CS-1 (see Figure S3 of the Supporting Information) indicated the presence of four N species. The lowest binding energy of 398.0 eV could be ascribed to $-NH_2$ interacting with Fe_3O_4, and the other three peaks at 398.8, 399.6, and 400.5 eV correspond to $-NH-COOCH_3$, $-NH_2$, and $-NH_3^+$ groups in CS, which are consistent with the results reported elsewhere.[23,24] The interaction between $-NH_2$ and Fe_3O_4 is assumed to serve as the cross-linking bridges and favor the stability of the CS shell coated onto the Fe_3O_4 core. Thus, we believed that, although the CS dosage of Fe_3O_4−CS-3 is much higher than Fe_3O_4−CS-2 during preparation, the same CS content of both composites may result from their same Fe_3O_4 amount and the CS only interacting with Fe_3O_4 is stable, while others will be rinsed by water.

Figure 2a shows the XRD patterns of Fe_3O_4 and Fe_3O_4−CS-1. The sharp, strong peaks with 2θ = 30.1°, 35.5°, 43.1°, 53.4°,

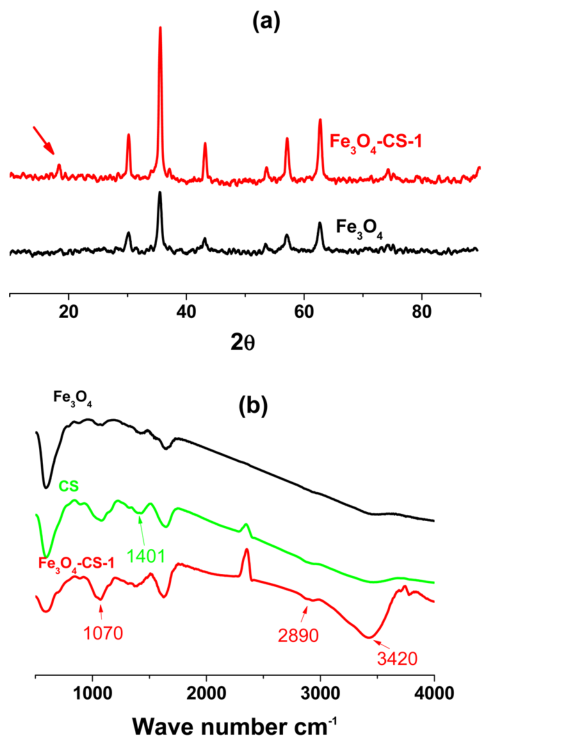

Figure 2. (a) XRD patterns of Fe_3O_4 and Fe_3O_4−CS −1 and (b) FTIR spectra of Fe_3O_4, CS, and Fe_3O_4−CS-1.

57.0°, and 62.6° proved that Fe_3O_4 was well-crystallized.[25] The XRD pattern of Fe_3O_4−CS-1 was very similar to that of the Fe_3O_4 nanoparticles, implying that the crystal Fe_3O_4 did not change during the solvothermal reaction with CS. In addition, a small peak at 2θ =20° indicated the presence of amorphous CS.[26]

FTIR spectra of Fe_3O_4, CS, and Fe_3O_4−CS-1 were shown in Figure 2b. The infrared (IR) spectrum of CS is characterized by the following absorption bands: ν(C−H) of the backbone polymer, around 2890 cm^{-1}; ν(C−O) of the primary alcoholic group, 1401 cm^{-1}; ν(C−O) of amide, 1070 cm^{-1}; and δ(N−H) of primary amine, around 3420 cm^{-1}. The IR spectrum of Fe_3O_4−CS-1 further demonstrated that CS was successfully coated onto nano-Fe_3O_4.

Another noteworthy observation is that, after reaction in such high temperatures, CS of weight average molecular weight (M_w) (38.13 × 10^4) would be gradually degraded into polymers of low M_w values (9.05 × 10^4), as measured via gel permeation chromatography (GPC) using a PL-GPC 50 chromatograph equipped with a refractive index detector (see Table S1 of the Supporting Information).

3.2. Effect of pH on Cu(II) Adsorption. Effect of equilibrium pH (pH_e) on adsorption of Fe_3O_4−CS for Cu(II) was studied by varying the initial pH range of 2−6. As shown in Figure 3, the adsorption of Cu(II) on Fe_3O_4−CS-1 increased

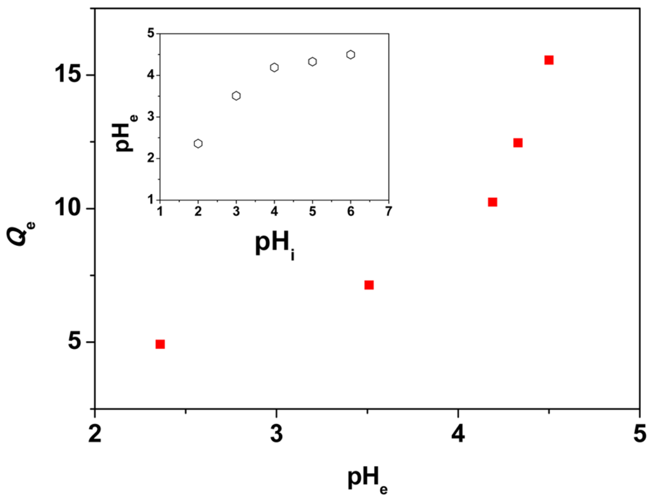

Figure 3. Effect of equilibrium solution pH on Cu(II) uptake of Fe_3O_4−CS-1. The initial concentration of Cu(II) was 50.0 mg/L.

with the increasing pH_e from 2 to 5, with the maximum capacity of 15.6 mg/g at pH_e 4.5. It is generally known that the $-NH_2$ groups are responsible for Cu(II) bindings. At acidic pH values, the amine group is protonated to some extent, which is unfavorable for Cu(II) adsorption because of the electrostatic repulsion. To avoid the possible precipitation of Cu(II), we set the optimum pH at 5.0 for further studies, where Fe_3O_4−CS is stable without any leaching of nano-Fe_3O_4 (see Figure S4 of the Supporting Information)

3.3. Adsorption Isotherms. Adsorption isotherms of Cu(II) on Fe_3O_4 and Fe_3O_4−CS at 25 °C and pH 5.0 are depicted in Figure 4a. Note that adsorption of Fe_3O_4 toward Cu(II) is negligible in the studied concentration ranges. Obviously, both Fe_3O_4−CS exhibited much higher capacity toward Cu(II) than the bulky Fe_3O_4 particles.

The obtained adsorption data were fitted using the Langmuir isotherm model

$$\frac{1}{Q_e} = \frac{1}{K_L Q_m C_e} + \frac{1}{Q_m} \quad (1)$$

where C_e is the equilibrium concentration, Q_e is the adsorptive capacity at equilibrium, and Q_m is the maximum adsorptive capacity (mg/g). It is shown that the Langmuir equation can well describe the isothermal Cu(II) adsorption by Fe_3O_4−CS samples, implying the monolayer coverage of Cu(II) ions. The maximum adsorptive capacity Q_m of Fe_3O_4−CS-1 reached 129.6 mg/g of beads (617.1 mg/g of CS; K_L = 1.68 × 10^{-3}; R^2 = 0.988), around 2 times that of Fe_3O_4−CS-2 (Q_m = 63.5 mg/g of beads; K_L = 4.05 × 10^{-3}; R^2 = 0.971). A much larger Q_m value of Fe_3O_4−CS-1 demonstrated that Fe_3O_4−CS-1 particles were better dispersed and exhibited more active sites than Fe_3O_4−CS-2, although the latter has higher CS content. To directly examine different dispersions of both composites, we carried out a DLS experiment on both samples, and the results shown in Figure S5 and Table S1 of the Supporting

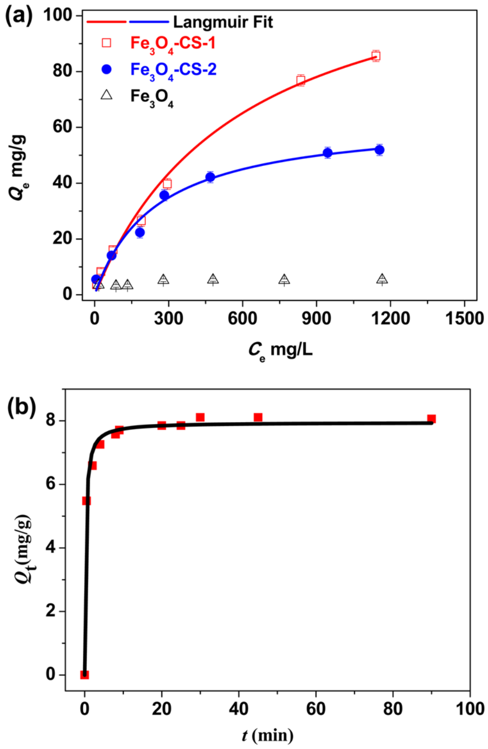

Figure 4. (a) Adsorption isotherms of Cu(II) on (black open triangles) Fe_3O_4, (red open squares) Fe_3O_4−CS-1, and (blue solid circles) Fe_3O_4−CS-2 at 25 °C and pH 5.0. (b) Adsorption kinetics of Cu(II) on Fe_3O_4−CS-1 at 25 °C and pH 5.0 [initial concentration of Cu(II) was 30 mg/L].

Information further supported the results from TEM images. In comparison to other magnetic CS adsorbents in reported work,[16,27] Fe_3O_4−CS-1 showed a notable high adsorptive capacity (617.1 mg/g of CS), which can be attributed to the nanosized distribution of the particles (200 nm). Note that such Fe_3O_4−CS also exhibited satisfactory adsorption toward other toxic metals, such as lead ions (see Figure S6 of the Supporting Information).

3.4. Adsorption Kinetics. Figure 4b showed the adsorption kinetic curve of Cu(II) onto Fe_3O_4−CS-1. Obviously, a fast initial Cu(II) adsorption was observed in the initial 5 min, and the adsorption equilibrium was achieved in 10 min. Such fast adsorption kinetics was very competitive for practical application. Comparatively, at least 10 h is required to reach the adsorption equilibrium of Cu(II) by the magnetic CS−cellulose beads,[9] as controlled by the intraparticle diffusion. Such fast adsorption of Fe_3O_4−CS-1 is mainly attributed to its finer particle size (nearly 200 nm in diameter) and thin CS shell, and we assume that the adsorption should not be controlled by intraparticle diffusion but by mass transport.[18,28] In addition, such fast kinetics was also consistent with that of a magnetic CS nanocomposite prepared by chemical grafting,[17] which also possesses a very thin CS shell. The pseudo-first-order model was employed to represent the kinetics data

$$\ln(q_e - q_t) = \ln q_e - k_1 t \tag{2}$$

where q_e and q_t represent the adsorptive capacities onto adsorbents (mg/g) at equilibrium and time t (min), respectively, and k_1 (g mg^{-1} min^{-1}) is the rate constant of the pseudo-first-order model. We obtained k_1 = 0.482 min^{-1} with the relative coefficient R^2 = 0.992.

3.5. Magnetic Separation. We characterized the magnetization curves of Fe_3O_4 and Fe_3O_4−CS-1 by a vibrating sample magnetometer (VSM), and the results are illustrated in Figure 5a. The saturation magnetization of Fe_3O_4 and Fe_3O_4−CS-1

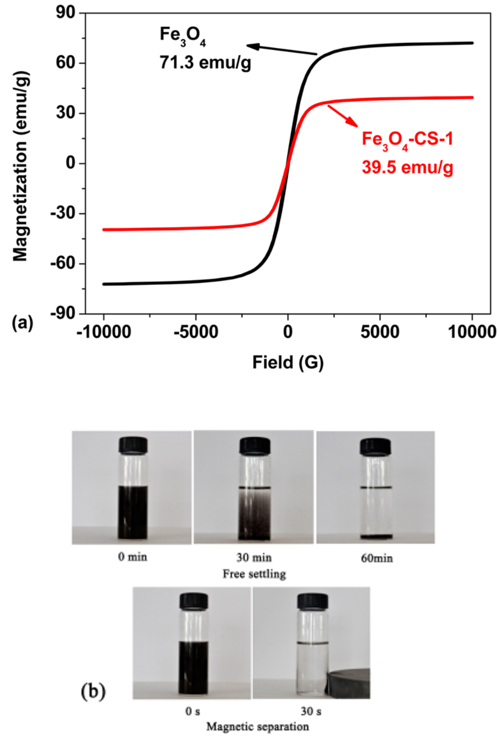

Figure 5. (a) Magnetization curves of Fe_3O_4 and Fe_3O_4−CS-1 at room temperature. (b) Separation of Fe_3O_4−CS-1 from water. Free settling and magnetic separation [magnetic field (MF) < 0.035 T; non-uniform magnetic field].

was about 71.3 and 39.5 emu/g, respectively. Because of the diamagnetics of CS, the saturation magnetization of Fe_3O_4−CS-1 was lower than that of Fe_3O_4 particles. Also, the interaction between the coated CS and Fe_3O_4 could also quench the magnetic moment.[29] We also examined the separation properties of Fe_3O_4−CS-1 from water in a low magnetic field. As shown in Figure 5b, Fe_3O_4−CS-1 can subside in water within 60 min and the presence of a low magnetic field (<0.035 T) favored a much faster sedimentation (within 30 s). It is generally known that the acting force of the magnetic field on the particles is directly proportional to the particle size.[30−32] As seen in Figure 1, the generally uniform (or monodisperse) particle size distribution of Fe_3O_4−CS-1 beads is favorable for fast sedimentation under low magnetic field.

3.5. Reusability. The reusability of Fe_3O_4−CS-1 was also examined through regeneration and cyclic adsorption. After regeneration by 0.01 M Na_2EDTA with the efficiency >97%, the adsorption capacity of Fe_3O_4−CS-1 was fully recovered, with the constant adsorption capacity in 6 continuous adsorption cycles (Figure 6). The excellent reusability renders us to believe that Fe_3O_4−CS-1 has great potential in decontamination of water from heavy metals.

 dx.doi.org/10.1021/am405562c | ACS Appl. Mater. Interfaces 2014, 6, 3421−3426

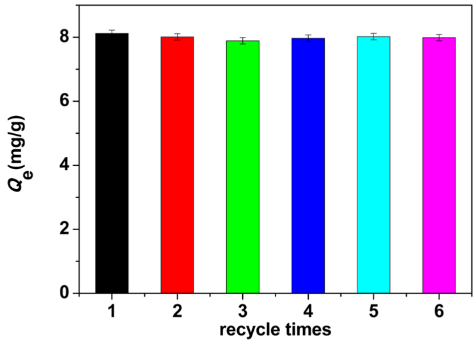

Figure 6. Adsorption capacity of Fe_3O_4−CS-1 for Cu(II) during cyclic experiments (initial concentration of 30 mg/L at pH 5.0).

4. CONCLUSION

Here, we presented a facile one-step process for *in situ* fabrication of magnetic CS beads Fe_3O_4−CS, and the as-obtained composite exhibited comparable high capacity and fast kinetics for copper removal. Moreover, it could be effectively recycled and reused in the presence of a low magnetic field. The magnetic CS Fe_3O_4−CS exhibits considerable potential in environmental remediation.

■ ASSOCIATED CONTENT

Supporting Information

TGA characterization, TEM images of Fe_3O_4 and Fe_3O_4−CS-3, XPS analysis, stability results, size distribution of the composites, GPC results, and lead adsorption isotherms (Figures S1−S6 and Tables S1−S2). This material is available free of charge via the Internet at http://pubs.acs.org.

■ AUTHOR INFORMATION

Corresponding Authors

*Telephone: +86-25-8968-0390. E-mail: bcpan@nju.edu.cn (B.P.).

*E-mail: esellu@nju.edu.cn (L.L.).

Notes

The authors declare no competing financial interest.

■ ACKNOWLEDGMENTS

This work was supported by the Natural Science Foundation of Jiangsu Province (BK 2012017 and 20130557) and the National Natural Science Foundation of China (NSFC) (51378249).

■ REFERENCES

(1) Matlock, M. M.; Howerton, B. S.; Atwood, D. A. Chemical precipitation of heavy metals from acid mine drainage. *Water Res.* **2002**, *36* (19), 4757−4764.

(2) Chen, Y.; Pan, B.; Li, H.; Zhang, W.; Lv, L.; Wu, J. Selective removal of Cu(II) ions by using cation-exchange resin-supported polyethyleneimine (PEI) nanoclusters. *Environ. Sci. Technol.* **2010**, *44* (9), 3508−3513.

(3) Wu, N.; Wei, H.; Zhang, L. Efficient removal of heavy metal ions with biopolymer template synthesized mesoporous titania beads of hundreds of micrometers size. *Environ. Sci. Technol.* **2012**, *46* (1), 419−425.

(4) Hunsom, M.; Pruksathorn, K.; Damronglerd, S.; Vergnes, H.; Duverneuil, P. Electrochemical treatment of heavy metals (Cu^{2+}, Cr^{6+}, Ni^{2+}) from industrial effluent and modeling of copper reduction. *Water Res.* **2005**, *39* (4), 610−616.

(5) Farooq, U.; Kozinski, J. A.; Khan, M. A.; Athar, M. Biosorption of heavy metal ions using wheat based biosorbents—A review of the recent literature. *Bioresour. Technol.* **2010**, *101* (14), 5043−5053.

(6) Cerino-Cordova, F. J.; Diaz-Flores, P. E.; Garcia-Reyes, R. B.; Soto-Regalado, E.; Gomez-Gonzalez, R.; Garza-Gonzalez, M. T.; Bustamante-Alcantara, E. Biosorption of Cu(II) and Pb(II) from aqueous solutions by chemically modified spent coffee grains. *Int. J. Environ. Sci. Technol.* **2013**, *10* (3), 611−622.

(7) Yan, H.; Yang, L.; Yang, Z.; Yang, H.; Li, A.; Cheng, R. Preparation of chitosan/poly(acrylic acid) magnetic composite microspheres and applications in the removal of copper(II) ions from aqueous. *J. Hazard. Mater.* **2012**, *229*, 371−380.

(8) Ngah, W. S. W.; Teong, L. C.; Hanafiah, M. Adsorption of dyes and heavy metal ions by chitosan composites: A review. *Carbohydr. Polym.* **2011**, *83* (4), 1446−1456.

(9) Rinaudo, M. Chitin and chitosan: Properties and applications. *Prog. Polym. Sci.* **2006**, *31* (7), 603−632.

(10) Liu, H. J.; Yang, F.; Zheng, Y. M.; Kang, J.; Qu, J. H.; Chen, J. P. Improvement of metal adsorption onto chitosan/*Sargassum* sp. composite sorbent by an innovative ion-imprint technology. *Water Res.* **2011**, *45* (1), 145−154.

(11) Zhou, Y.; Yang, D.; Chen, X.; Xu, Q.; Lu, F.; Nie, J. Electrospun water-soluble carboxyethyl chitosan/poly(vinyl alcohol) nanofibrous membrane as potential wound dressing for skin regeneration. *Biomacromolecules* **2008**, *9* (1), 349−354.

(12) Arias, J. L.; Reddy, L. H.; Couvreur, P. Fe_3O_4/chitosan nanocomposite for magnetic drug targeting to cancer. *J. Mater. Chem.* **2012**, *22* (15), 7622−7632.

(13) Kievit, F. M.; Veiseh, O.; Bhattarai, N.; Fang, C.; Gunn, J. W.; Lee, D.; Ellenbogen, R. G.; Olson, J. M.; Zhang, M. Q. PEI−PEG−chitosan−copolymer-coated iron oxide nanoparticles for safe gene delivery: Synthesis, complexation, and transfection. *Adv. Funct. Mater.* **2009**, *19* (14), 2244−2251.

(14) Klepka, M. T.; Nedelko, N.; Greneche, J. M.; Lawniczak-Jablonska, K.; Demchenko, I. N.; Slawska-Waniewska, A.; Rodrigues, C. A.; Debrassi, A.; Bordini, C. Local atomic structure and magnetic ordering of iron in Fe−chitosan complexes. *Biomacromolecules* **2008**, *9* (6), 1586−1594.

(15) Jung, J. H.; Lee, J. H.; Shinkai, S. Functionalized magnetic nanoparticles as chemosensors and adsorbents for toxic metal ions in environmental and biological fields. *Chem. Soc. Rev.* **2011**, *40* (9), 4464−4474.

(16) Liu, Z.; Wang, H.; Liu, C.; Jiang, Y.; Yu, G.; Mu, X.; Wang, X. Magnetic cellulose−chitosan hydrogels prepared from ionic liquids as reusable adsorbent for removal of heavy metal ions. *Chem. Commun.* **2012**, *48* (59), 7350−7352.

(17) Liu, X. W.; Hu, Q. Y.; Fang, Z.; Zhang, X. J.; Zhang, B. B. Magnetic chitosan nanocomposites: A useful recyclable tool for heavy metal ion removal. *Langmuir* **2009**, *25* (1), 3−8.

(18) Chang, Y. C.; Chen, D. H. Magnetic chitosan nanoparticles: Studies on chitosan binding and adsorption of Co(II) ions. *J. Colloid Interface Sci.* **2005**, *283* (2), 446−451.

(19) Sun, S. H.; Zeng, H.; Robinson, D. B.; Raoux, S.; Rice, P. M.; Wang, S. X.; Li, G. X. Monodisperse MFe_2O_4 (M = Fe, Co, Mn) nanoparticles. *J. Am. Chem. Soc.* **2004**, *126* (1), 273−279.

(20) Sun, S. H.; Zeng, H. Size-controlled synthesis of magnetite nanoparticles. *J. Am. Chem. Soc.* **2002**, *124* (28), 8204−8205.

(21) Hou, Y. L.; Yu, J. F.; Gao, S. Solvothermal reduction synthesis and characterization of superparamagnetic magnetite nanoparticles. *J. Mater. Chem.* **2003**, *13* (8), 1983−1987.

(22) Liu, Q. S.; Yang, C. L.; Chen, J. A.; Jiang, B. W. Preparation of monodisperse highly-magnetic biodegradable chitosan nanospheres with core−shell structure. *J. Controlled Release* **2011**, *152*, E250−E252.

(23) Dambies, L.; Guimon, C.; Yiacoumi, S.; Guibal, E. Characterization of metal ion interactions with chitosan by X-ray photoelectron spectroscopy. *Colloids Surf., A* **2001**, *177* (2−3), 203−214.

(24) Shen, C. S.; Shen, Y.; Wen, Y. Z.; Wang, H. Y.; Liu, W. P. Fast and highly efficient removal of dyes under alkaline conditions using

magnetic chitosan−Fe(III) hydrogel. *Water Res.* **2011**, *45* (16), 5200−5210.
(25) Ji, J. H.; Ji, S. F.; Yang, W.; Li, C. Y. Preparation and application of magnetic Fe_3O_4 nano-crystalline. *Process. Chem.* **2010**, *22* (8), 1566−1574.
(26) Liu, Z.; Wang, H.; Li, B.; Liu, C.; Jiang, Y.; Yu, G.; Mu, X. Biocompatible magnetic cellulose−chitosan hybrid gel microspheres reconstituted from ionic liquids for enzyme immobilization. *J. Mater. Chem.* **2012**, *22* (30), 15085−15091.
(27) Chen, Y. W.; Hu, J.; Wang, J. L. Kinetics and thermodynamics of Cu(II) biosorption on to a novel magnetic chitosan composite bead. *Environ. Technol.* **2012**, *33* (20), 2345−2351.
(28) Liu, J. F.; Zhao, Z. S.; Jiang, G. B. Coating Fe_3O_4 magnetic nanoparticles with humic acid for high efficient removal of heavy metals in water. *Environ. Sci. Technol.* **2008**, *42* (18), 6949−6954.
(29) Vanleeuwen, D. A.; Vanruitenbeek, J. M.; Dejongh, L. J.; Ceriotti, A.; Pacchioni, G.; Haberlen, O. D.; Rosch, N. Quencehing of magnetic-moments by ligand−metal interactions in nanosized magnetic metal clusters. *Phys. Rev. Lett.* **1994**, *73* (10), 1432−1435.
(30) Kelland, D. R. Magnetic separation of nanoparticles. *IEEE Trans. Magn.* **1998**, *34* (4), 2123−2125.
(31) Jiang, W.; Chen, X.; Niu, Y.; Pan, B. Spherical polystyrene-supported nano-Fe_3O_4 of high capacity and low-field separation for arsenate removal from water. *J. Hazard. Mater.* **2012**, *243*, 319−325.
(32) Yavuz, C. T.; Mayo, J. T.; Yu, W. W.; Prakash, A.; Falkner, J. C.; Yean, S.; Cong, L.; Shipley, H. J.; Kan, A.; Tomson, M.; Natelson, D.; Colvin, V. L. Low-field magnetic separation of monodisperse Fe_3O_4 nanocrystals. *Science* **2006**, *314* (5801), 964−967.